J. Membrane Biol. 184, 283–290 (2001)
DOI: 10.1007/s00232-001-0089-y

The Journal of
Membrane
Biology

Fluid Secretion in *Rhodnius* Upper Malpighian Tubules (UMT): Water Osmotic Permeabilities and Morphometric Studies

C.S. Hernández[a], A. M. Gutiérrez[a], A. Vargas-Janzen[b], F. Noria[b], E. González[b], V. Ruiz[a] , G. Whittembury[a]
[a]Instituto Venezolano de Investigaciones Científicas, IVIC, P.O. Box 21827, Caracas 1020-A, Venezuela
[b]Facultad de Medicina, UCV, Caracas, Venezuela

Received: 15 August 2001

Abstract. We have measured the osmotic permeability of the basolateral cell membrane (P_{os}^{cb}) and compared it with the transepithelial permeability (P_{os}^{te}) to calculate the paracellular (P_{os}^{p}) permeability of the upper malpighian tubules (UMT) of the 5th instar of *Rhodnius prolixus* under several experimental conditions, namely, at rest and after stimulation to secrete with 5-HT, each under control conditions (no treatment), after treatment with pCMBS, and after addition of pCMBS and DTT. Secretion rate is negligible at rest. During stimulation mean secretion rate is 43.5 nl/cm^2 sec. Secretion is severely curtailed by pCMBS and fully restored by DTT. $P_{os}^{cb} = 9.4$ (resting, control); 5.8 (control + pCMBS); 10.7 (control + pCMBS + DTT); 20.6 (stimulated, control); 14.7 (stimulated + pCMBS); 49.1 (stimulated + pCMBS + DTT) ($\times 10^{-4}$ cm^3/cm^2 sec Osm). Calculated P_{os}^{p} are higher than the transcellular permeability, P_{os}^{c}, at rest and after stimulation. Electron micrograph morphometry of UMT sections show that cells significantly decrease their volume after stimulation. Lateral intercellular space (LIS) and basolateral extracellular labyrinth (BEL) are barely discernible at rest. LIS and BEL are widely dilated in stimulated UMT. Thus, ions have restricted access to the deep and narrow basolateral cell membrane indentations at rest, but they have ready access to cell membrane indentations after stimulation, because of the opening of LIS and BEL. These findings are discussed in relation to isosmotic secretion. The rate-limiting step for paracellular movement is located at the smooth septate junctions.

Correspondence to: G. Whittembury; email: gwhitt@ivic.ve
Symbols and abbreviations: 5-HT, 5-hydroxytryptamine; DTT, dithiothreitol; pCMBS, parachloromercuribenzenesulphonate; LIS, lateral intercellular space; BEL, basolateral extracellular labyrinth

Key words: Epithelial morphometry — Water channels — Fluid Secretion — *Rhodnius prolixus* — Malpighian tubules — Secretion

Preface

In 1953, as a medical student in Peru, I (GW) wanted to learn transport biophysics, which John Merrill had suggested I could do at A. K. Solomon's Biophysics Laboratory at Harvard; therefore, my tutor Carlos Monge had me study Ussing's papers [11, 20, 21], which I did with relish. I went to Boston in 1957 with a Rockefeller Foundation Fellowship and met Ussing in 1959, on his way to a Gordon Conference in New Hampshire, which Solomon (who took kind care of me) had arranged I could attend. I remember Solomon asking Ussing whether he wanted to phone Mrs. Ussing about his safe arrival in Boston. Ussing said: "Annamarie knows I am driving with you. As you are known to use top speed in your Porsche, she will be more at ease if we phone her from New Hampshire". There, Ussing presented his "two membrane model" of epithelial transport [12], which explained so many of our findings at Solomon's and at Giebisch's laboratories in the kidney tubule, that Giebisch and I decided we should think in Ussing's terms. Giebisch and I kept a close friendship since, inspired, I believe, by the gentle way in which Ussing always talked to us. Since then, Ussing directly influenced my scientific career. A few examples follow.

I realized (in 1965) I could make sense of the ratio of 10 of transtubular to cell membrane osmotic permeability in *Necturus* proximal tubules, if there were a paracellular shunt for water [27] as well as for ions [36]. But could I visualize the shunt? In 1970, at Ullrich's superb meeting in Schloss Reinhartshausen, Ussing showed that Ba^{2+} deposited in frog skin tight

junctions opened by apical urea [22, 23]. Following that we showed that La^{3+} deposited in the proximal tubule junctions, showing they were normally open [33]; and that intravenous urea created in the collecting duct a situation similar to the frog skin [23], namely, that big solutes like raffinose permeated along these otherwise tight junctions [7]. Later, using solvent drag [2], we demonstrated paracellular water flow in leaky epithelia [35], which I presented in one of the elegant Alfred Benzon Symposia that Ussing and friends organized at the Royal Danish Academy of Sciences and Letters. I could feel that Ussing had conveyed his inquisitive, firm but kind attitude to his colleagues. There, Ussing and his sweet wife Annamarie kindly took me to dine, more than once, at their home where music and literature completed, with utmost finesse, a pleasant evening. As Ussing also tackled isosmotic secretion [14, 24], it is fitting that this paper deals with this subject that motivated long discussions between us, as was the case for the 4 decades I had known him and tried to follow his example. I end this preface on a note about Ussing's intuition. He realized [11] that the net osmotic to diffusive water permeability ratio led to an estimate of an equivalent pore radius for the water pathways [18, 19], but that there was a limit as the pore radius approaches that of the water molecule, which has turned out to be the case [1, 8, 30].

Introduction

The blood-sucking insect *Rhodnius prolixus* Stål (Hemiptera, Reduvidae) has 4 Malpighian tubules whose upper end (UMT) suddenly secretes when stimulated by 5-HT [15]. UMT of the 5th instar are 20–25 mm long, 80–90 μm in diameter, 50–65 nl/cm in volume and with a peritubular basement membrane area of 0.025–0.029 cm^2. They do not secrete at rest, but stimulated with 5-HT, secretion rates are 50 nl/cm^2 of basement membrane area per second or more [9, 15, 28]. An important question concerns whether water moves mainly via transcellular or paracellular pathways or both. Some have shown the importance of the transcellular pathway [16, 17] while others underscore the paracellular pathway [9, 28]. To clear these points, several questions must be answered. (i) The transepithelial osmotic permeability has been assessed [16], but that of the cell membranes has not. This is critical to complete an equivalent circuit of hydraulic resistances for this epithelium. (ii) Given the considerable changes in secretory rate from rest to the peak of stimulation, it is important to know whether there are morphological changes during secretion, whether the cell membrane water permeabilities and cell volume vary during secretion. This would indicate water movement across the cell membrane. If the latter were the case we should ascertain whether water moves through the lipid bilayer part of the membrane or through water channels, as in the mammalian proximal tubule [29], or through both. The present paper addresses some of these questions.

Materials and Methods

UMT of the fifth instar of *Rhodnius*, dissected out of the insect, were used [9, 28]. The insects were bred and kept in the laboratory at 28°C and 95% humidity in incubators, were fed (across a rubber membrane) once a month throughout their instars with heparinized (2 units/ml) sheep blood. The UMT are transparent with few cytoplasmic concretion bodies. UMT of insects fed with hen's blood are opaque, with concretions, which made them cumbersome for some studies [25].

Bathing Solutions

Solutions were used right after being bubbled with 95% O_2/5% CO_2. (a) IR, insect Ringer with composition (in mmol/l), NaCl, 129; KCl, 8.6; NaH_2PO_4, 4.3; $NaHCO_3$, 10.2; $CaCl_2$, 2.0; glucose, 34; alanine, 3; pH, 7.35–7.45; osmolality, 340 mOsm/kg, i.e., isosmotic to the insect haemolymph [15]. (b) MBS, isosmotic mannitol bathing solution, with composition similar to IR, except that 129 mmol/l NaCl were replaced by 240 mmol/l mannitol. Preliminary experiments indicated mannitol, sucrose and raffinose as cell membrane-impermeant solutes. We used mannitol [7]. (c) HMBS, hyperosmotic bathing solution (440 mOsm/kg) prepared by adding 100 mOsm/kg mannitol to MBS. Osmolalities were measured by freezing-point depression. To stimulate secretion, 5-HT to a concentration of 2 μmolar was added to the bath [15]. Where indicated, pCMBS to a concentration of 2 mmolar and DTT to a concentration of 5 mmolar were added to the bath.

Secretion Rate

Briefly, an UMT was transferred to a drop of 75–100 μl of oxygenated IR at 25°C kept under mineral oil. Some 20 mm of the blind end were left in the IR drop. The cut end was drawn out and secured around a hydrophilic pin 10 mm away to collect secretion and perfusate. The UMT blind end was taken out of the IR drop and was cannulated with a sharp perfusion pipette containing IR. IR was perfused through the lumen at 10 nl/min. The spherical drop of perfusate and tubule secretion were measured every 5 min using a dissecting microscope with a micrometer scale. Secreted volume (v) was calculated from the total spherical volume appearing at the cut end (after subtraction of the perfusion volume), ($v = \pi d^3/6$). Secretion rate was expressed per cm^2 of basement membrane surface area, calculated from the tubule length and diameter [9].

Osmotic (Net) Permeabilities, P_{OS}

The osmotic permeability coefficient is defined as $P_{os} = L_p\, RT/V_w$, where L_p is the hydraulic permeability coefficient; R the gas constant, T the absolute temperature and V_w the molar volume of water. Superscripts to P_{os} indicate the location of the measurement: P_{os}^{cb} = basolateral cell membrane; P_{os}^{ca} = apical cell membrane; P_{os}^{cyt} = cytosolic; P_{os}^{c} = transcellular = $1/[(1/P_{os}^{cb}) + (1 + P_{os}^{ca}) + (1 + P_{os}^{cyt}]$; P_{os}^{p} = paracellular; P_{os}^{te} = transepithelial permeability = $(P_{os}^{c}) + (P_{os}^{p})$.

Basolateral Cell Membrane Osmotic Permeability, P_{os}^{cb}

P_{os}^{cb} is measured from the rate of cell volume change per unit basement membrane area per unit time, per unit concentration difference, which is set up between cell and bath by the sudden change from MBS to HMBS. The method has been detailed [4, 29, 32]. Here we used 1-to 2-mm long UMT segments held with micropipettes in a chamber leaving a useful UMT length of 0.2–0.4 mm between pipettes. UMT were bathed in IR (equilibrated with 95% O_2/5% CO_2) at 25°C on an inverted microscope. Tubule lumen was filled with sudan black-stained oil. The microscope was adapted with a TV camera and an image processor with its output fed onto a memory oscilloscope [32]. From the records, tubule and cell volume were calculated as a function of time. Five minutes before the osmotic step, IR was replaced by MBS where secretion is absent even in stimulated tubules. To produce the osmotic step, HMBS was replaced about the tubule in less than 80 msec. Cells shrunk. After 20 sec, MBS was returned to the chamber using the same method. Shrinking and swelling curves were used to calculate P_{os}^{cb}. Tubule diameter was checked periodically with an image splitter [4].

Transmission Electron Microscopy

Eleven UMT were dissected, immersed in oxygenated IR for 15 min in the resting (nonstimulated) condition. Then they were prefixed in Karnovsky's fluid [10, 28] adjusted to 340 mOsm/kg with sucrose and NaCl, 70% and 30% of the required total. Another 11 UMT were dissected and immersed in oxygenated IR to which 5-HT had been added to stimulate secretion. They were similarly prefixed after 15 min. Then, UMT were washed in 0.1 M phosphate buffer, postfixed in 1% OsO_4 isosmolar to IR; dehydrated in a graded ethanol series to end in propylene oxide. They were infiltrated and embedded in polybed 812. Ultrathin transversal sections were double stained with uranyl acetate and lead citrate. They were then examined in a 400 T Philips electronmicroscope at 80 KV.

Morphometry

Serial micrographs of each transversal section of each UMT (normal to its length) were taken at 2800× magnification, copied to 8400×. Each mosaic was built by setting up together some 12–14 photographs that completed the circumference. Several mosaics of whole sections of each tubule were prepared for their morphometric study [26]. Chemicals were from Sigma Chemical (St. Louis, MO).

Results

Influence of 5-HT, pCMBS and DTT on UMT Secretory Rate

Figure 1 shows secreted volume vs time of 9 experiments in each curve. UMT were bathed in oxygenated IR. They were already lumen-perfused for 10 minutes before $t = 0$. Secretion is ~0 at rest (▲). Addition of 5-HT at $t = -10$ min stimulates secretion to levels of ~60 µl/cm^2 at min 20 (□). Mean secretion rate was 43.5 nl/cm^2 of basement membrane area per second. For symbols •, pCMBS had been added to the bath at $t = -20$ min; then, 5-HT was added at $t = 0$. Mean secretion rate is 18.2 nl/cm^2 sec, indicating that pCMBS curtailed secretion. At $t = 22$ min DTT was added to the bath. The experiment continues as ○. Secretion is now 69.3 nl/cm^2 sec. Thus DTT counteracts pCMBS action as secretion is above the levels of the stimulated tubules.

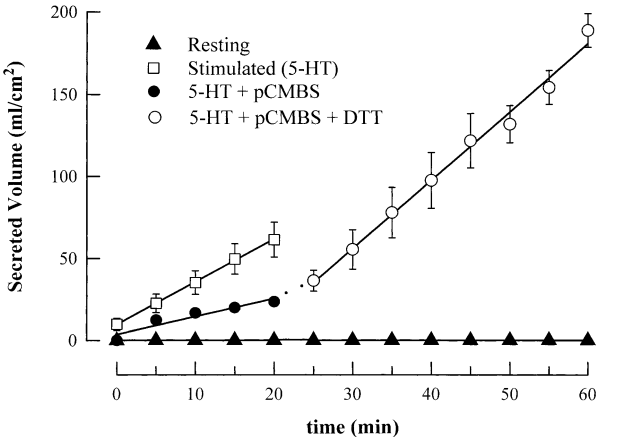

Fig. 1. Secreted volume of lumen perfused UMT. Mean ± SEM of 9 UMT in each condition plotted vs time. (i) (▲) = resting UMTs. Mean secretion rate = 3×10^{-4} nl/cm^2 sec (i.e., undetectable). (ii) □ = stimulated UMT. Mean secretion rate = 43.5 nl/cm^2 sec. The intercept ($t = 0$) is 9.6 nl/cm^2, as 5-HT had been added at $t = -10$ min. (iii) • , at $t = -20$ min pCMBS had been added to the bath. Then at $t = 0$, 5-HT was added. Mean secretion rate = 18.2 nl/cm^2 sec. Thus secretion was clearly curtailed as compared to □. Then at $t = 22$ min DTT was added. The experimental line continues in ○. Now, secretion rate = 69.3 nl/cm^2 sec. Thus, the effect of pCMBS is reversed.

Influence of 5-HT, pCMBS and DTT on P_{os}^{cb}

Figure 2 shows typical experiments to measure P_{os}^{cb} in resting (*A*) and in 5-HT-stimulated UMT (*B*). Both figure parts show three curves. Control (no additions); after addition of pCMBS (+pCMBS); and after addition of pCMBS and DTT (+DTT). UMT was bathed in MBS. At $t = 0$, HMBS replaces MBS. Cells shrink. Only 3 sec of the trace are shown. Notice (Fig. 2*A*) that curve +pCMBS drops the least, +DTT drops the most, while the Control curve occupies an intermediate position. Not shown is that after 20 sec MBS was restored. Cells completely recovered their original volume. P_{os}^{cb} was calculated from the shrinking and from the recovery curves. Values coincided and, pooled together, are given in Table 1. P_{os}^{cb} in resting UMT was 9.4 in units of 10^{-4} cm^3/cm^2 of basement membrane area · sec osmolar. With pCMBS it was 5.8 (same units), and with pCMBS that had been then treated with DTT, it was 10.7 (same units). Thus, DTT reversed pCMBS action as 10.7 almost doubles 5.8. In stimulated UMT (Fig. 2*B*) the rate and degree of shrinking produced by HMBS was larger

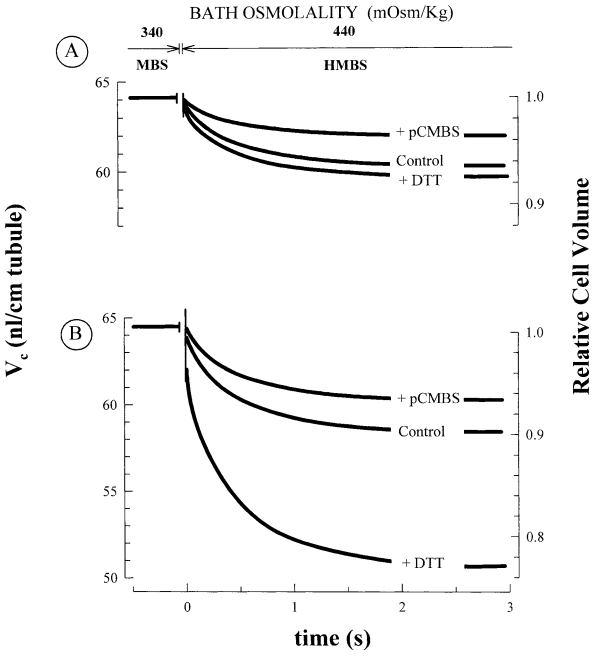

Fig. 2. Typical experiments to measure P_{os}^{cb}. Plots of UMT cell volume, V_c, *vs.* time (seconds). UMT were equilibrated in isosmotic mannitol bathing solution, MBS. At $t = 0$ s, MBS was replaced by hyperosmotic MBS (HMBS). Cells shrink. Only 3 sec of the traces are shown. After 20 sec (not shown) MBS was restored. Cells swelled and recovered their original volume. P_{os}^{cb} was calculated from the shrinking and from the recovery curves for each experiment (*see* Methods). (*A*) Resting UMT. Three curves are shown. *Control* (no additions); *+pCMBS* (pCMBS added at min −20); *+DTT* (pCMBS added at min −20 and DTT at min −5). (*B*) 5-HT-stimulated UMT. Same convention as in *A*.

than in the resting tubules. In the stimulated controls (no additions except for 5-HT), P_{os}^{cb} was 20.6. With pCMBS, P_{os}^{cb} was 14.7, smaller than the controls (same units). With DTT, P_{os}^{cb} was 49.1, a value significantly larger than the controls and than the pCMBS-treated UMT. Thus DTT reverses the inhibitory action of pCMBS on P_{os}^{cb}. For the same condition, P_{os}^{cb} was larger in the stimulated than in the resting UMT. Thus, in the controls, P_{os}^{cb} increases from 9.4 to 20.6; with pCMBS, from 5.8 to 14.7, and with DTT, from 10.7 to 49.1 (same units), respectively.

Table 1 also gives calculated transcellular permeabilities (the sum of apical, cytosolic and basolateral permeabilities in series), P_{os}^{c}, which were similar in the stimulated and in the resting UMT, because of the large cytoplasmic hindrance to flow [31]. Since we have no measured values for P_{os}^{ca}, we assumed it has the same value as the measured basolateral permeability. A $P_{os}^{cyt} = 2 \times 10^{-4}$ cm^3/cm^2 of basement membrane area · sec · osmolar was used [31]. P_{os}^{te} are taken from [16]. P_{os}^{p} values are calculated by subtracting P_{os}^{c} from P_{os}^{te}. Notice that neither P_{os}^{te} nor P_{os}^{p} change with stimulation.

Morphometric Analyses

Figures 3*A* and 3*B* are mosaics of resting and stimulated UMT. 3*C* and 3*D* are larger magnifications. In resting UMT, neighboring cells are closely apposed with barely visible intercellular spaces (LIS) and basolateral indentations that leave only a "virtual" BEL (Fig. 3*A* and 3*C*) [c.f. 28], while (3*B* and 3*D*), in stimulated UMT, LIS and BEL are dilated, except for the normal septate junctions [13, 28].

Cell Parameters

Table 2 shows that cell area per cross section was smaller in stimulated than in resting UMT (2908 μm^2, resting, *vs.* 2726 μm^2; stimulated, $p < 0.01$), due to cell height reduction from 18.0 μm to 13.7 μm ($p < 0.01$) in the part not occupied by microvilli. Microvilli height does not change. In fact, cells diminish their volume with stimulation, since UMT length does not change with stimulation.

Apical Cell Membrane Amplification

It is known that microvilli and basolateral cell membrane indentations increase cell membrane area. Secretory rates and permeabilities as given above (per cm^2 of basement membrane area), do not take these amplifications into consideration. The following data pool together resting and stimulated UMT, since there are no differences between these conditions.

Table 1. Water osmotic permeabilities (P_{os}, in 10^{-4} cm^3/cm^2 of basement membrane area sec osmolar) of UMT, and of rabbit proximal straight tubules (PST).

Osmotic permeabilities, P_{os}	P_{os}, Resting UMT	P_{os}, Stimulated UMT	PST[a]
P_{os}^{cb}	9.4 ± 1.1 (8)	20.6 ± 1.7 (38)	90
P_{os}^{cb} + 2mM pCMBS	5.8 ± 0.6 (5)	14.7 ± 1.6 (34)	7
P_{os}^{cb} + 2mM pCMBS + 5mM DTT	10.7 ± 1.5 (11)	49.1 ± 6.0 (33)	100
P_{os}^{te} (taken from [16])	23–43	20–42	77
P_{os}^{c} (calculated from[b])	2	2	32
P_{os}^{P}	21–41	18–40	45

[a] PST values taken from [4].
[b] Calculated using $P_{os}^{cyt} = 2 \times 10^{-4}$ cm^3/cm^2 sec osmolar [31].
Number of experiments is given in parentheses.

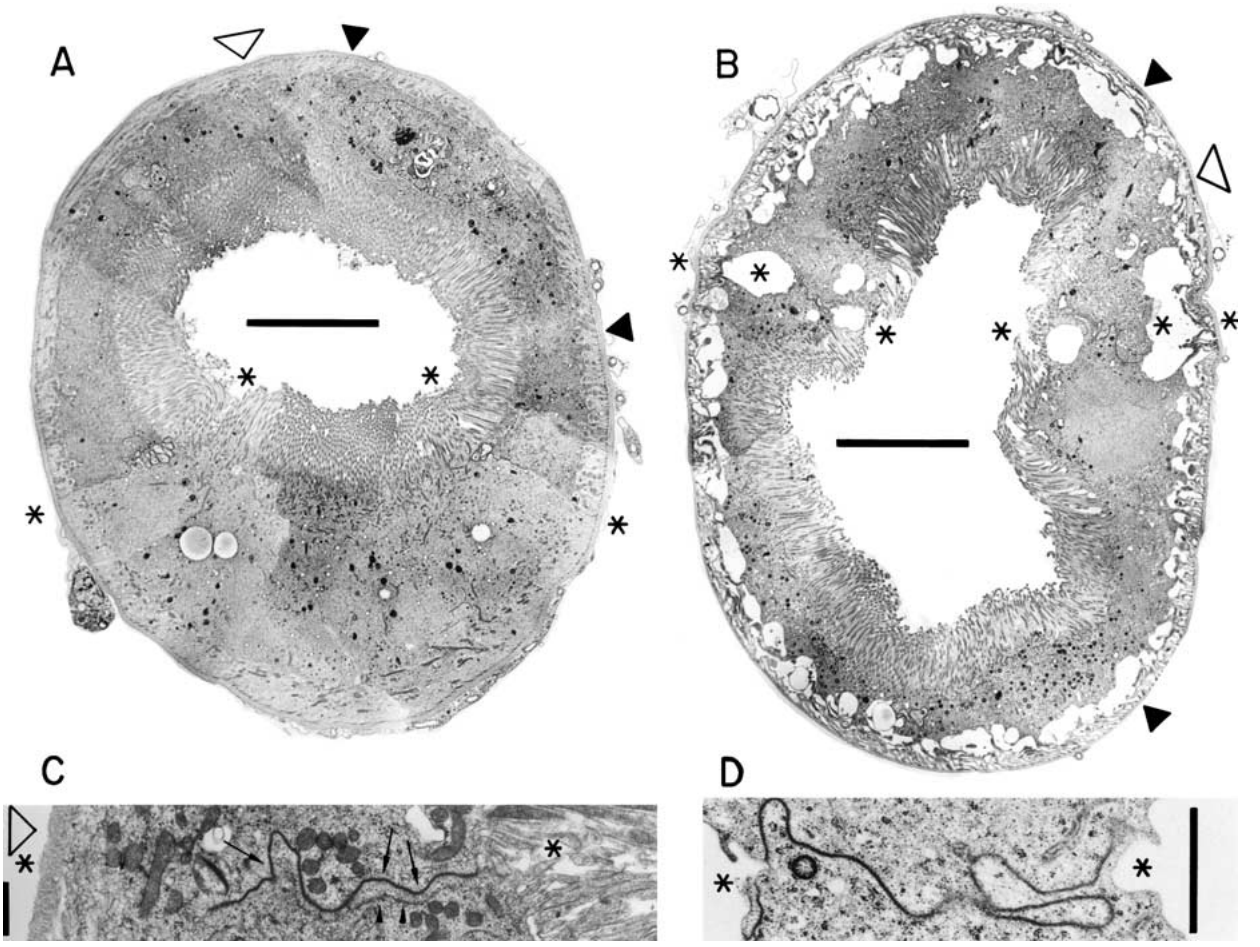

Fig. 3. *A* and *B* are mosaics of resting and stimulated UMT sections, respectively. The mosaic components may be seen. Scale bar 10 μm. The thick basement membrane surrounds the tubule (Δ). As 2 cells form the circumference, there are two LIS marked ** at their lumen and basement membrane end. The septate junction begins right where the microvilli finish. They end about the middle of the cytoplasmic height. In *A* (resting UMT) (▲) near the basement membrane indicates regions where basolateral infoldings can be best discerned but without a prominent extracellular space between infoldings and basement membrane. In *B* (stimulated UMT) * shows greatly dilated regions of LIS. Septate junctions appear normal [13, 28]. BEL between basolateral cell membrane infoldings and basement membrane are clearly visible (▲). *C* and *D* are details of part of LIS of resting and stimulated UMT, respectively. Scale bar 1 μm. Septate junctions appear normal (arrows). LIS dilations * are prominent in *D*.

Apparent lumen area (taken as a flat cylinder, without considering microvilli indentations), $S_{v,al}$ = 0.027 ± 0.003 $\mu m^2/\mu m^3$ UMT volume. Real apical cell membrane area (with microvilli indentations), $S_{v,ca}$ = 2.57 ± 0.41 $\mu m^2/\mu m^3$ tubule volume. Thus, microvilli amplify apical cell membrane area 97×, (= 2.57/0.027), per μm^2 of apical area; or 42×, per μm^2 of basement membrane area.

Basolateral Cell Membrane Amplification

In resting UMT, septate junction width is 164 ± 15 Å; its mean height is 7.5 μm [9], and intercellular space (LIS) length, 12–14 μm [9]. LIS has an average width of 333 Å in 50% of the measurements and in the other 50% one of 600 Å [*c.f.* 28]. Figures 3*A* and *C* show resting UMT.

Basement membrane area, $S_{v,bm}$ (taken as a cylinder) did not change from rest to stimulation. Pooled data = 0.061 ± 0.008 $\mu m^2/\mu m^3$ of tubule volume. Despite changes in the width of intercellular and basolateral spaces after stimulation, no difference was observed in the boundary length, *B*, between resting (239) and stimulated tubules (278) $\mu m/\mu m^3$ of UMT volume. The pooled data = 258 $\mu m/\mu m^3$. Basolateral cell membrane area, $S_{v,BEL}$, was 0.46 (resting) and 0.52 (stimulated) $\mu m^2/\mu m^3$ of UMT volume. Pooled $S_{v,BEL}$ = 0.49 $\mu m^2/\mu m^3$ of UMT volume. Therefore, there is no change in real intercellular and basolateral cell membrane area, and therefore neither in cell membrane amplification between resting and stimulated UMT, despite large changes in extracellular space volume. Therefore, we have pooled BEL amplification together. BEL amplification is then 8×, i.e., 8.0 ± 0.6 μm^2 of real basolateral cell membrane

Table 2. Morphometric parameters in UMT at rest and after stimulation. Mosaics of eleven resting and eleven stimulated UMT were analyzed.

	Resting (n = 11)	Pooled Data	Stimulated (n = 11)	Difference p
Cellular and apical				
Lumen area*, μm^2	539 ± 95		777 ± 121	NS
Cell Area*, μm^2	2908 ± 214		2726 ± 207	< 0.01
Total cell height, μm	18.0 ± 0.9		13.7 ± 0.8	< 0.001
Microvilli height, μm	5.6 ± 0.3	5.45 ± 0.42	5.3 ± 0.2	NS
Apical amplification, referred to lumen surface, $S_{v,ca}/S_{v,al}$ ($\mu m^2/\mu m^2$)		97 ± 10		
Apical amplification, referred to basement membrane surface, $S_{v,ca}/S_{v,bm}$ ($\mu m^2/\mu m^2$)		4.42 ± 5		
Intercellular and basolateral				
Intercellular Boundary length, B, ($\mu m/\mu m^3$)	239 ± 41	258 ± 41	278 ± 26	NS
Basolateral cell membrane area $S_{v,BEL}$, ($\mu m^2/\mu m^3$)	0.46 ± 0.06	0.49 ± 0.07	0.52 ± 0.05	NS
Basal extracellular labyrinth (BEL) amplification, $S_{v,BEL},/S_{v,bm}$, ($\mu m^2/\mu m^2$)	7.5 ± 0.4	8.0 ± 0.6	8.5 ± 0.4	NS
BEL space volume**, $V_{v,BEL}$, ($\mu m^3/\mu m^3$)	0.0064 ± 0.0005		0.0786 ± 0.0097	< 0.001

* per tubule cross section.
** between basolateral cell membrane infoldings and basement membrane.

area/μm^2 of basement membrane area (taken as a cylinder), for the measured average UMT diameter of 66 μm after fixation and dehydration. In vivo 5th instar UMT diameters range from 80 to 90 μm.

BEL Volume

With stimulation, BEL volume (between basolateral cell surface infoldings and basement membrane), $V_{v,BEL}$, increases from a "virtual" resting value of 0.0064 $\mu m^3/\mu m^3$ (i.e., 0.64% of tissue volume, [*c.f.* 28] to a value of 0.0786 $\mu m^3/\mu m^3$, i.e. 7.86 or ~8% of tissue volume. We have not detected variation in septate junction width or length with stimulation (Fig. 3*B* and 3*D*). The rest of LIS and BEL expanded under stimulation. As mentioned above, this change is not due either to alteration in the length of B between adjacent cells, or to changes in the surface area of the basal infoldings, $S_{v,BEL}$ from resting to stimulation. It seems related to "cell shrinkage". The volume of ~8% reached by BEL, $V_{v,BEL}$, after stimulation is not due to a uniform expansion of LIS (Fig. 3*B*). To give a figure, its mean width is of some 0.5 μm. As just mentioned, after stimulation, BEL increases while there is a decrease in cell volume. This is perhaps related to the increased microscopic transparency of UMT, which can be noticed (when held with pipettes to perform P_{os}^{cb} measurements in vitro) within seconds of 5-HT addition.

Discussion

Six fundamental observations stem from this work, namely: (i) There is a sizable resting P_{os}^{cb} that is inhibited (to ~60%) by the sulfhydryl reagent pCMBS, an inhibition fully reversed by the sulfhydryl-reducing agent DTT. (ii) Stimulated P_{os}^{cb} is larger and is also inhibited (to ~70%) by pCMBS, an action also reverted by DTT. (i) and (ii) suggest that UMT may possess, like the mammalian proximal kidney tubule, cell membrane water channels [29]. In fact, a new protein, RP-mip, which may act as a water channel, has been described and cloned in apical and basolateral cell membranes of UMT [6]. (iii) For any given condition (resting-control *vs.* stimulated-control; resting-pCMBS *vs.* stimulated-pCMBS; resting-DTT *vs.* stimulated-DTT), stimulated P_{os}^{cb} are larger than resting P_{os}^{cb}. Basolateral cell membrane areas, $S_{v,BEL}$, are equal in stimulated and in resting UMT (Table 2). Therefore, an alternative explanation to this difference in P_{os}^{cb} is observation (iv), which is as follows. LIS width has been functionally measured with probes as a slit with an equivalent width of 11.0 Å [9] both at rest and after stimulation. Morphologically, LIS, barely discernible at rest (width 333–600 Å) opens to a space with an average width of ~0.5 μm under stimulation. In addition, basal extracellular labyrinth (BEL) volume, which is ~0.6% at rest, opens with stimulation to occupy ~8% of tubule volume. Thus, after stimulation all basolateral cell membrane water channels would be exposed and accessible to the peritubular-probing anisosmotic solution present, after solution change to measure P_{os}^{cb}, at the external aspect of the basement membrane. That would not be the case for all the water channels in the resting UMT where only those closer to the basement membrane would be accessible to the probing-solution constituents. The narrow and long "virtual" basolateral spaces would hinder diffusion,

delaying the time that the anisosmotic solution would take to reach its target site at the cell membrane level. For example, it can be calculated that the time for 95% equilibration ($t_{0.95}$) for mannitol diffusing in a slit along LIS in the resting UMT would be 0.6–0.8 sec, i.e. near 1 sec.[1] (v) Resting and stimulated P_{os}^{cb} values with pCMBS are 5.8 and 14.7×10^{-4} cm^3/cm^2 sec osmolar, respectively (Table 1). These values could be taken to represent the P_{os}^{cb} of the lipid part of the cell membrane. If the accessibility argument mentioned above holds (14.7/5.8 = 2.5), the basolateral cell membranes would be 2.5 times more available to the basal probes in the stimulated than in the resting UMT. P_{os}^{cb} values increase in stimulated UMT after DTT to 49.1. This would represent the full P_{os}^{cb} of the basolateral cell membrane. Comparable values for the mammalian PST are 7 (pCMBS) and 100 (DTT, same units). Thus in resting and stimulated UMT an important part of the permeability may be due to water flow through the bilayer part of the membrane. (vi) The high values of P_{os}^{cb} at rest, but particularly during stimulation, insure quick cell volume changes secondary to the osmotic changes that may occur during secretion.

We now consider arguments concerning the paracellular pathway in the light of observation (iv). Solvent drag of molecules of different diameters during secretion in UMT is best explained by solvent drag through an 11.0 Å-wide slit, as a monotonic function fits best the resting and stimulated data at widely different secretion rates [9]. LIS is made of the 7–8 μm-long septate junction and the 12–14 μm-long LIS proper [9]. The present observation (iv) shows no discernible variation in septate junction length or width during stimulation, while LIS dilates considerably in stimulated UMT. Thus, it may be concluded that the rate-limiting step for solvent drag must be the septate junction, the invariant structure during secretion, and not LIS, which should offer little or no restriction to sieving at different rates of secretion. Values of P_{os}^{p} (Table 1) do not change from resting to stimulated UMT. This also indicates that widening of LIS proper and of BEL does not directly influence paracellular resistance to osmotic induced water flow. These values of P_{os}^{p} are much larger than the transcellular values, pointing out that water should cross the epithelium more easily through the paracellular pathway.

As is the case of other isosmotic transporting epithelia, we are still far from understanding the mechanisms that move water in these structures. Studies on solvent drag of graded-sized molecules lead to the conclusion that most water flow must be paracellular [9, 28]. The critical question is, what is the role of the water channels deduced from the present observations and now described in UMT [6]. The quick volume changes after 5-HT stimulation would indicate that just prior to secretion some contractile or other mechanism induces cell volume changes resulting in opening of LIS and BEL, so that all elements at the basolateral cell membrane level are fully accessible to the ions (and water) that must permeate from the haemolymph to the basolateral cell aspect to be introduced in the cells by mechanisms that have yet to be ascertained, as have to be those that relate cellular and paracellular water flows.

E.G. is a Visiting Scientist at IVIC. It is a pleasure to thank Dr. G. M. Villegas for her help with the e.m. studies; also Mr. J. Mora and Mr. A. Cazorla for their enthusiastic help with equipment; to Mr. L.S. Alvarez and Mrs. Lelis Ochoa for their help with the drawings; and to Mrs. T. Omaira Silva and Mr. Mardonio Díaz for great help with the electronmicrographs. This work was partially supported by CONICIT, Fundación Polar and CDCH of UCV

References

1. Agre, P. 2000. Homer W. Smith Award lecture. Aquaporin water channels in kidney. *J. Am. Soc. Nephrol.* **11:**764–777
2. Andersen, B., Ussing, H.H. 1957. Solvent drag on non electrolytes during osmotic flow through isolated toad skin and its response to antidiuretic hormone. *Acta Physiol. Scand.* **39:**228–239
3. Bruins H.R. 1929. Coefficient of diffusion in liquids. *In:* International Critical Tables. **5:**71, Mc Graw Hill, New York.
4. Carpi-Medina, P., Whittembury G. 1988. Comparison of transcellular and transepithelial water osmotic permeabilities (P_{os}) in the isolated proximal straight tubule (PST) of the rabbit kidney. *Pfluegers Arch.* **412:**66–74
5. Crank, H. 1959. The mathematics of diffusion. Clarendon Press, Oxford.
6. Echevarría, M., Ramírez-Lorca, R., Hernández, C.S., Gutiérrez, A.M., Méndez-Ferrer, S., González, E., Toledo-Aral, J.J., Ilundáin, A.A., Whittembury, G. 2001. Identification of a new water channel (RP-mip) in the malpighian tubules of the insect *Rhodnius prolixus*. *Pfluegers Arch.* **442:**27–34.
7. González, E., Leal-Pinto, E., Pérez-González, M., Whittembury G. 1980. Abnormal transtubular permeability to raffinose during intravenous infusión of urea and of mannitol in the intact dog kidney. *Pfluegers Arch.* **383:**165–171.
8. Gutierrez A., González E., Echevarría M., Hernández C.S., Whittembury G. 1995. The proximal straight tubule (PST) basolateral cell membrane water channel: selectivity characteristics. *J. Membrane Biol.* **143:**189–197.
9. Hernández C.S., González E., Whittembury G. 1995. The paracellular channel for water secretion in the upper segment

[1] An equation for diffusion in a plane sheet [5] is: $[1-(C_e/C_b)] = (8/\pi^2) \cdot \exp(-D_s\pi^2 t/x^2)$, in which (C_e/C_b) is the ratio of the mannitol concentration in the interspaces to that in the bath, D_s is the mannitol diffusion coefficient within the channel. $D_s = D_s^\circ \cdot S_{ds} \cdot F_{ds}$ i.e., the free solution diffusion coefficient times the steric and drag coefficients S_{df} and F_d for mannitol diffusion. Diffusion hindrance for mannitol is $= S_{ds} \cdot F_{ds} = (1-\alpha) \cdot (1-1.004\alpha+0.418\alpha^3-0.210\alpha^4-0.169\alpha^5)$ [9, Eqn 2]. Mannitol has a diameter of 8.0 Å. For an 11.0-Å wide slit, which represents the effective width of the structure where mannitol diffuses [9], $\alpha_{Mannitol} = 8.0/11.0 = 0.727272...$ Therefore, $S_{ds}F_{ds} = 0.0921$; $D_s^\circ = 0.72 \times 10^{-5}$ cm^2/sec [3]; $D_s = 0.0663 \times 10^{-5}$ cm^2/sec. Taking a representative BEL length of 5 μm [28] and a LIS length of 12–14 μm [9], the time ($t_{0.95}$) it would take for 95% equilibration within these slit-shaped channels would be 0.11sec and 0.61–0.83sec for mannitol in BEL and LIS, respectively.

of the malpighian tubule of *Rhodnius Prolixus*. *J. Membrane Biol*. **148:**233–242.
10. Karnovsky, M.J. 1965. A formaldehyde-glutaraldehyde fixative of high osmolality for use in electron microscopy. *J. Cell Biol*. **27:**137A.
11. Koefoed-Johnsen, V., Ussing, H.H. 1953. The contribution of diffusion and flow to the passage of D_2O through living membranes. *Acta Physiol. Scand*. **28:**60–76.
12. Koefoed-Johnsen, V., Ussing, H.H. 1958. The nature of the frog skin potential. *Acta Physiol. Scand*. **42:**298–308.
13. Lane, N.J., Skaer, H. leB. 1980. Intercellular junctions in insect tissues. *Adv. Insect. Physiol*. **15:**35–213.
14. Larsen E.H., Nedergaard S., Ussing H.H. 2000. Role of lateral intercellular space and sodium recirculation for isotonic transport in leaky epithelia. *Rev. Physiol. Biochem. Pharmacol*. **141:**153–212.
15. Maddrell, S.H.P. 1980. Characteristics of Epithelial transport in Malpighian Tubules. *Curr. Topics in Membr. & Transport*. **14:**427–463.
16. O'Donnell, M.J., Aldis, S.K., Maddrell, S.H.P. 1982. Measurements of osmotic permeability in the Malpighian tubules of an insect, *Rhodnius prolixus* Stal. *Proc. R. Soc. London B*. **216:**267–277.
17. O'Donnell, M.J., Maddrell, S.H.P. 1983. Paracellular and transcellular routes for water and solute movements across insect epithelia. *J. Exp. Biol*. **106:**231–253.
18. Pappenheimer, J.R., Renkin, E.M., Borrero, L.M. 1951. Filtration, diffusion and molecular sieving through peripheral capillary membranes. *Am. J. Physiol*. **167:**13–46.
19. Solomon, A.K. 1968. Characterization of biological membranes by equivalent pores. *J. Gen. Physiol*. **51:**335s–364s.
20. Ussing, H.H. 1949. The distinction by means of tracers between active transport and diffusion. *Acta Physiol. Scand*. **19:**43–56.
21. Ussing, H.H. 1949. Transport of ions across cellular membranes. *Physiol. Rev*. **29:**127–155.
22. Ussing, H.H. 1971. Structure and Function of Epithelia. *In:* Electrophysiology of Epithelial Cells. Symposia Medica Hoechst. G. Giebisch, editor. pp 3–16. F.K. Schattauer Verlag, Stuttgart-New York.
23. Ussing, H.H., Windhager, E.E. 1964. Nature of shunt-path and active sodium transport path through frog skin epithelium. *Acta Physiol. Scand*. **61:**484–504.
24. Ussing H.H., Eskesen, K. 1989. Mechanism of isotonic water transport in glands. *Acta Physiol. Scand*. **136:**443–454.
25. Vargas-Janzen, A., Whittembury, G., Hernández, C.S., Sánchez, F., Villegas, G.M., González, E. 1996. Microconcresiones de calcio en túbulos de Malpighi de *Rhodnius*. Ultraestructura y morfometría. *Revista Soc. Venezol. Ciencias Morfológicas* **2:**3–40.
26. Weibel, E.R., Bolender, R.P. 1973. Stereological techniques for electron microscopic morphometry. *In:* Principles and Techniques of Electron Microscopy **3:**237–296 M.A. Hayat, editor. Van Nostrand, New York.
27. Whittembury, G. 1967. Sobre los mecanismos de absorción en el túbulo proximal del riñón. *Acta Cient. Venezol*. **18:**(Suppl. 3) 43–56.
28. Whittembury, G., Biondi, A.C., Paz-Aliaga, A., Linares, H., Parthe, V., Linares, N. 1986. Transcellular and paracellular flow of water during secretion in the upper segment of the Malpighian tubule of *Rhodnius prolixus*: solvent drag of molecules of graded size. *J. Exp. Biol*. **123:**71–92.
29. Whittembury, G., Carpi-Medina, P., Gonzalez, E., Linares, H. 1984. Effect of parachloromercuribenzensulfonic acid and temperature on cell water osmotic permeability of proximal straight tubules. *Biochim. Biophys. Acta* **775:**365–373
30. Whittembury, G., González, E., Gutiérrez, A.M., Echevarría, M., Hernández, C.S. 1997. Length of the selectivity filter of aquaporin-1. *Biology of the Cell*. **89:**299–306.
31. Whittembury, G., Hill, A. 2000. Coupled transport of water and solutes across epithelia. *In:* D. Seldin, G. Giebisch, eds. The Kidney, Physiology and Pathophysiology, 3rd edition, Chapter 14, pp 341–362, Lippincott Williams & Wilkins, New York.
32. Whittembury, G., Lindemann, B., Carpi-Medina, P., González, E., Linares, H. 1986. Continuous measurements of cell volume changes in single kidney tubules. *Kidney Int* **30:**187–19133.
33. Whittembury, G., Rawlins, F.A. 1971. Evidence of paracellular pathways for ion flow in the kidney proximal tubule: electron microscopic demonstration of lanthanum precipitate in the tight junction. *Pfluegers Archiv*. **330:**302–309.
34. Whittembury, G., Verde de Martínez, C., Linares, H., Paz-Aliaga, A. 1980. Solvent drag of large solutes indicates paracellular water flow in leaky epithelia. Proc. Roy. Soc. London, B. **211:**63–81.
35. Windhager, E.E., Boulpaep, E.L., Giebisch, G. 1967. Electrophysiological studies in single nephrons. *In:* Proc 3rd. Int Congress of Nephrol. Washington DC. 1966. vol 1, pp 35–47 Basel, Karger.